Article

Core–Shell Structures Prepared by Atomic Layer Deposition on GaAs Nanowires

Veaceslav V. Ursaki [1,2], Sebastian Lehmann [3], Victor V. Zalamai [1], Vadim Morari [4], Kornelius Nielsch [3], Ion M. Tiginyanu [1,2] and Eduard V. Monaico [1,*]

[1] National Center for Materials Study and Testing, Technical University of Moldova, 2004 Chisinau, Moldova
[2] Academy of Sciences of Moldova, 2001 Chisinau, Moldova
[3] Institute for Metallic Materials (IMW), Leibniz Institute of Solid State and Materials Research (IFW Dresden), Helmholtzstr. 20, 01069 Dresden, Germany
[4] Institute of Electronic Engineering and Nanotechnologies "D. Ghitu", 2028 Chisinau, Moldova
* Correspondence: eduard.monaico@cnstm.utm.md

Abstract: GaAs nanowire arrays have been prepared by anodization of GaAs substrates. The nanowires produced on (111)B GaAs substrates were found to be oriented predominantly perpendicular to the substrate surface. The prepared nanowire arrays have been coated with thin ZnO or TiO_2 layers by means of thermal atomic layer deposition (ALD), thus coaxial core–shell hybrid structures are being fabricated. The hybrid structures have been characterized by scanning electron microscopy (SEM) for the morphology investigations, by Energy Dispersive X-ray (EDX) and X-ray diffraction (XRD) analysis for the composition and crystal structure assessment, and by photoluminescence (PL) spectroscopy for obtaining an insight on emission polarization related to different recombination channels in the prepared core–shell structures.

Keywords: nanowires; coaxial core–shell structures; anodization; atomic layer deposition; photoluminescence spectroscopy; emission polarization

Citation: Ursaki, V.V.; Lehmann, S.; Zalamai, V.V.; Morari, V.; Nielsch, K.; Tiginyanu, I.M.; Monaico, E.V. Core–Shell Structures Prepared by Atomic Layer Deposition on GaAs Nanowires. *Crystals* **2022**, *12*, 1145. https://doi.org/10.3390/cryst12081145

Academic Editor: Giancarlo Salviati

Received: 13 July 2022
Accepted: 11 August 2022
Published: 15 August 2022

Publisher's Note: MDPI stays neutral with regard to jurisdictional claims in published maps and institutional affiliations.

Copyright: © 2022 by the authors. Licensee MDPI, Basel, Switzerland. This article is an open access article distributed under the terms and conditions of the Creative Commons Attribution (CC BY) license (https://creativecommons.org/licenses/by/4.0/).

1. Introduction

Semiconductor nanowires and core–shell structures prepared on their basis are important building blocks for nano-electronic and micro-electronic devices. A large area of core–shell applications are related to photodiodes and photovoltaics, demonstrating significant advantages over planar structures and other device configurations in terms of radial charge collection and cost reduction, reduced reflection of injected light, and improving efficiency based on positional carrier separation [1–5]. Nanophotonics [6–10], non-linear optics and plasmonics [11,12], thermoelectrics [13], recognition of biomolecules, and biosensing [14] are among important applications of semiconductor quasi-one-dimensional core–shell structures. Among many arrays of core–shell nanowires, those with ZnO and TiO_2 shells are widely explored for various applications [5,6,15,16].

Apart from wide band gap materials, relatively narrow band gap materials, such as Si [2,7,17,18] and GaAs [19–22], were used as cores in core–shell structures. Enhanced responsivity was demonstrated on n-ZnO/p-Si radial heterojunction nanowire photodiodes in both ultraviolet (UV) and visible ranges, the photoresponsivity being larger than that of a planar thin film diode (PD) due to the efficient carrier separation and collection with improved light absorption [2,17,18]. In comparison with Si which has indirect band gap, III–V materials, such as GaAs, InP, and InAs, exhibit a direct band gap, which offers them some advantages for building optoelectronic devices. In general, III–V semiconductors have higher electron mobility than Si. GaAs and related III–V materials offer the highest energy conversion efficiency in photovoltaic devices.

In most of the prepared core–shell structures, the nanowire arrays are oriented perpendicularly to the substrate material. However, technological methods have been recently

developed for the preparation of GaAs nanowires oriented either perpendicularly or parallel to the initial GaAs substrate by a cost-effective electrochemical etching [23,24].

Core–shell structures with ferromagnetic shells have been prepared on the basis of these nanowires by means of electrochemical deposition, and the anisotropy of their magnetic properties has been investigated [23]. An infrared photodetector was also demonstrated [24]. Preparation of core–shell arrays with both perpendicular and parallel orientations with respect to the wafer surface is expected to enlarge the possibilities for controlling polarization of light detected or light emitted with such kind of structures. Spectacular morphologies of porous semiconductor compounds obtained via anodization and use of specific photolithographic masks to force the growth of pores parallel to the surface in self-organization mode were reported in a recent review paper [25]. Moreover, electrochemistry proved to be a cost-efficient and effective technology for the fabrication of core–shell arrays composed from Pt nanotubes embedded in semiconductor matrices [26].

As concerns the deposition techniques, atomic layer deposition (ALD) is an extremely valuable technique for growing with high accuracy conformal ultrathin films for planar device structures, as well as for fabricating core–shell structures, since the excellent surface conformation of ALD coatings makes it ideally suited for coating complex nanostructures [27]. ALD coatings provide high stability to complicated functional nanostructures resulting in improved performance of devices in such applications as photovoltaics, electrochemical energy storage, photo- and electrochemical devices, etc. [28]. Note that most of the above cited core–shell structures have been produced with ALD technologies.

Previous investigations demonstrated a polarization-sensitive characteristic of the photoluminescence recorded parallel and perpendicular to the long axis of semiconductor nanowires and core–shell structures, including those with GaAs core, which, in many cases, but not always, was explained in terms of large dielectric contrast between the free-standing nanowires and surrounding environment [29–38].

Although optical properties of core–shell nanowires with GaAs core [29,30], as well as those of ZnO nanowires [33], including the polarization characteristics, have been studied in previous papers, the polarization characteristics of ZnO shells on GaAs nanowires have not been explored.

The goal of this paper is to prepare core–shell structure by means of ALD deposition of ZnO and TiO_2 shells on GaAs nanowire arrays fabricated by anodization of GaAs substrates, to assess their optical quality be means of photoluminescence characterization, and to investigate the polarization characteristics of the observed luminescence bands.

2. Materials and Methods

ZnO and TiO_2 shells have been deposited by atomic layer deposition on GaAs nanowires.

GaAs nanowires oriented perpendicularly to the GaAs substrate were prepared by anodization of n-type (111)B-oriented Si-doped GaAs wafers, acquired from Mateck GmbH (Juelich, Germany), with a free electron concentration of 2×10^{18} cm^{-3}. The samples were cleaved into 1×1 cm^2 parts and were sonicated in acetone for 10 min, rinsed in distilled water and dried, before the anodization. They were also subjected to wet chemical etching in HCl/H_2O with a ratio of (1:3) for 2 min in order to remove the native oxide from the surface. The follow-up anodization was carried out in 1 M HNO_3 electrolyte at applied anodic potential of 4 V in a cell with three electrodes configuration. The schematics of the electrochemical setup was described in detail previously [39]. A piece of GaAs sample with a surface of 1 cm^2 served as working electrode, while a mesh from Pt wire with the total surface of 6 cm^2 was used as a counter electrode. A saturated Ag/AgCl was used as a reference electrode. Etching for 15 min resulted in a 45 μm thick nanostructured layer containing GaAs nanowires.

ZnO and TiO_2 were deposited using a thermal ALD reactor Veeco Savannah S200 from Veeco Instuments Inc. (Plainview, New York, USA) equipped with a disk-like chamber (diameter = 300 mm, height = 7 mm). Diethylzinc (DEZ) was used as the Zn precursor, $TiCl_4$ was used as the Ti precursor and deionized water (H_2O) was used as the oxygen

source. High-purity N_2 was used as the carrier gas and the chamber was kept at a flow rate of 20 sccm during the ALD reaction process. The optimized pulse and purge times were 0.03/60/0.03/60 s and 0.2/120/0.015/120 s for one ALD deposition cycle of ZnO ($DEZ/N_2/H_2O/N_2$) and TiO_2 ($TiCl_4/N_2/H_2O/N_2$), respectively. Due to lower reactivity of $TiCl_4$ with H_2O, an exposure time of 60 s with closed valve was added to fully allow the precursors to react. The chamber temperature was 150 °C for both ZnO and TiO_2 deposition.

It was found that 30 ms and 200 ms pulse time for DEZ and $TiCl_4$, respectively, are enough to saturate the surface [40]. In respect to the large surface area of the samples the exposure times were kept low and the purge times high to ensure the self-limiting character of the ALD-process. The growth rate of ZnO and TiO_2 was determined to be around 0.16 nm/cycle by measuring the thickness of Si-wafers using a spectroscopic ellipsometer (Ellipsometer, SENpro) as was reported elsewhere [41,42].

The morphology of the prepared samples was studied using a LEO-ZEISS Gemini 1530 (ZEISS, Jena, Germany) scanning electron microscope (SEM), equipped with EDX detector-analyzer. X-ray diffraction analysis was performed with a Philips X-Pert MPD System with Cu-Kα_1 radiation.

The photoluminescence (PL) was excited by a 325 nm He-Cd laser, the samples being mounted on the cold station of an LTS-22-C-330 optical cryogenic system. For unpolarized measurements, the excitation laser beam at 30 mW power was focused on the frontal surface of the sample with a nanowire array to a spot of about 2 mm in diameter, resulting in the excitation power density of about 1 W/cm^2. The emission was analyzed in a quasi-backscattering geometry through a double SDL-1 spectrometer. The signal from a FEU-106 photomultiplier with SbKNaCs photocathode working in a photon counting mode when measuring the emission in the UV and visible range and a FEU-62 photomultiplier with silver-cesium-oxygen when measuring the emission in the near IR range was introduced in an IBM computer. The spectral resolution was better than 1 meV. Apart from unpolarized measurements, investigations with PL emission polarized along the nanowires or in the radial direction, were performed by using Glan–Thompson analyzers, as schematically illustrated in Figure 1a,b, respectively. In such a case, the GaAs substrate was masked with a black foil to avoid its excitation. Apart from that, the power of the excitation beam was reduced and it was focused with an objective lens on the nanowire array. The emission comes from a large amount of nanowires in the array, both from the core and from the shell.

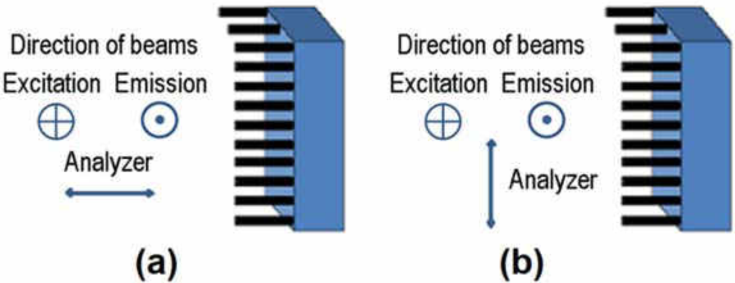

Figure 1. Schematics of polarized PL measurement with polarization along the nanowires (**a**) and polarization in the radial direction (**b**).

3. Results

The SEM image of a GaAs nanowire array fabricated by anodizing (111)B substrates in 1 M HNO_3 electrolyte for 15 min, is presented in Figure 2a. One can see that the nanowires with the length of 45 µm are oriented predominantly perpendicularly to the substrate surface [37]. The XRD pattern (Figure 2b) was measured frontally from the nanowire array produced on the substrate, it being collected both from the nanowire array and from the substrate, since the nanostructured layer containing GaAs nanowires is 45 µm thick, while the penetration of the Cu-Kα_1 radiation in the sample is of several hundreds of micrometers. The pattern is compared to a database XRD fingerprint obtained from a GaAs powder [43]. The predominance of (111) and (333) reflexes in the XRD pattern is indicative of the (111)B

crystallographic orientation of the sample. No reflexes from other phases, except the zinc blende GaAs are observed in the pattern, which suggests that the GaAs wires are of high crystalline quality similar to the substrate.

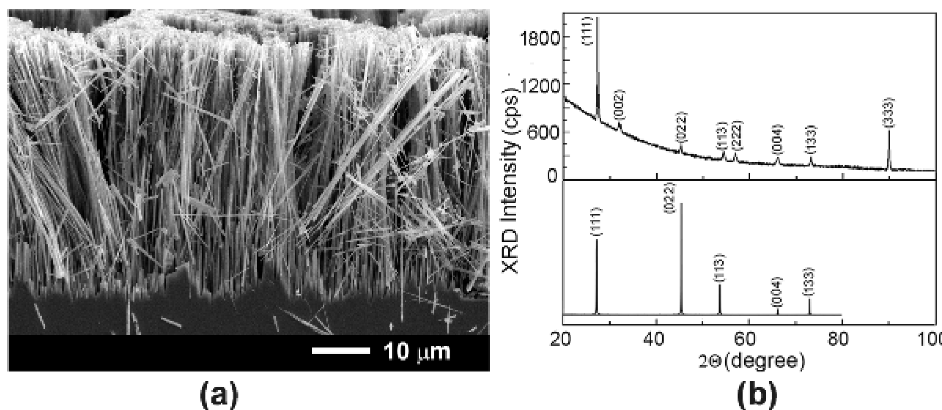

Figure 2. (**a**) Cross-section SEM image of a GaAs nanowire array produced by anodizing a GaAs substrate with (111)B crystallographic orientation; (**b**) XRD analysis of a GaAs nanowire array (upper part), compared to a database XRD fingerprint (lower part).

The morphology of TiO_2 and ZnO coatings on GaAs nanowires is shown in Figure 3. The thickness of coatings is estimated to be around 50 nm with a growth rate of 0.16 nm/cycle for a number of 310 cycles. It is supposed that the deposition starts with growing islands which are closing to conformal film with increasing cycle number. However, such kind of growth is also influenced by the roughness of the GaAs nanowires surface, which is not perfectly cylindrical along the nanowire axis, due to some current oscillations occurring during the anodization process. As a result, the morphology of coatings is bumpy. Apart from that, due to the high aspect ratio of nanowires they exhibit a tendency to agglomerate in bundles. Several effects may be influencing this behavior, such as electrostatic interaction between nanowires, non-uniform distribution of germination centers for initiation of anodization on the initial surface of the substrate, and stirring of the electrolyte during anodization. These effects may be even more pronounced during the ALD coating.

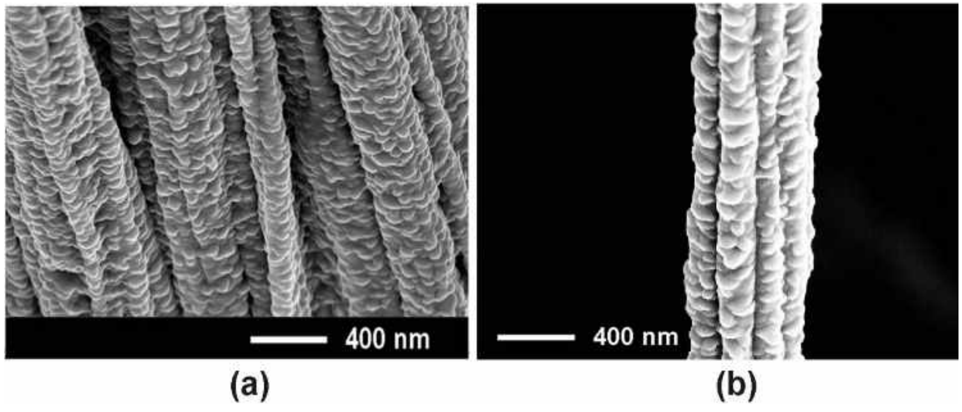

Figure 3. (**a**) SEM image of a GaAs nanowire array coated with a TiO_2 layer; (**b**) SEM image of a GaAs nanowire bundle coated with a ZnO layer.

The results of EDX analysis of an array of GaAs nanowires coated with TiO_2 by ALD measured in the direction parallel to the substrate, i.e., perpendicular to the nanowires, are presented in Figure 4. The carbon impurity was excluded from calculations, since its concentration is determined with large errors due to its low atomic number (6) in the periodic table. On the other hand, this leads to increasing errors in the determination of

other elements up to several at%. Anyway, the results show a nearly equal concentration of Ga and As, and a ratio of the atomic percentage of oxygen to titanium around 2.

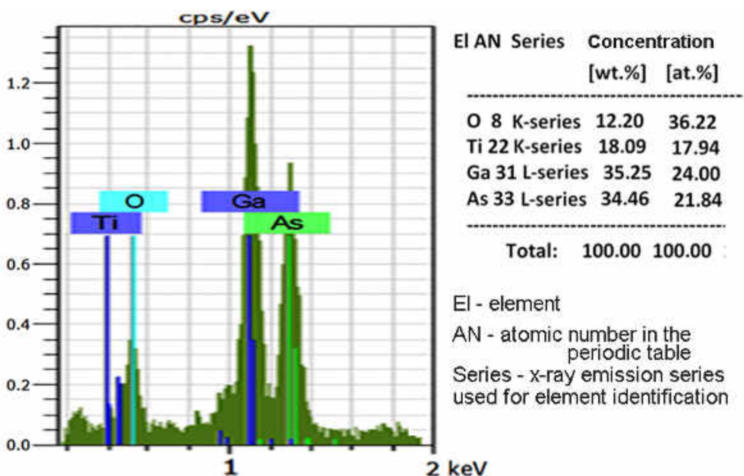

Figure 4. EDX analysis of a GaAs nanowire array coated with TiO_2 by ALD.

Further investigations are focused on the photoluminescence spectra of ZnO coatings on GaAs nanowires (Figure 5). The emission in the UV spectral range comes from the ZnO shell, while that in the IR range is from the GaAs core. The PL spectrum of the GaAs core of nanowires consists of three PL bands centered at 1.486 eV, 1.360 eV, and 1.310 eV, as deduced from Figure 5a. It was previously suggested that the high energy band at 1.486 eV is related either to donor–acceptor pair (DA) recombination [44–46], or to conduction band to Si_{As} acceptor transition [47,48], i.e., with shallow recombination centers, while the band at 1.360 eV was attributed either to arsenic-vacancy related complex [45], or to a gallium-vacancy related complex [47], or to Cu_{Ga} centers [46]. The full width at half maximum (FWHM) of the bands at 1.486 eV and 1.360 eV is 70 meV and 85 meV, respectively. Such a width is usual for donor–acceptor pair recombination involving distant pairs. The FWHM of the weak intensity band at 1.310 eV is much larger (220 meV). It could be related to some structural defects, such as dislocations. However, the nature of this band remains unclear, additional investigations being needed to through light on this issue.

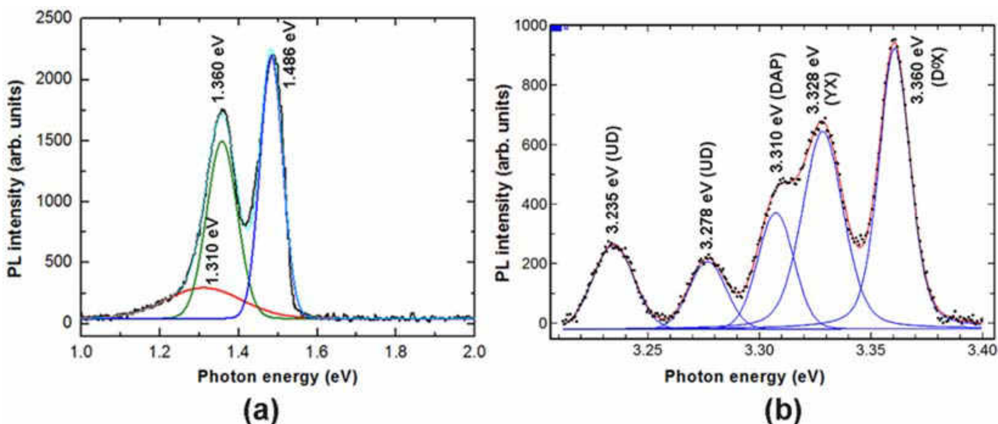

Figure 5. Unpolarized PL spectra of a GaAs nanowire array coated with a thin ZnO layer measured at 10 K in the IR spectral range (**a**), and in the UV range (**b**).

The emission from the ZnO shell consists of a 3.360 eV band and a series of lower energy bands at 3.328 eV, 3.310 eV, 3.278 eV, and 3.235 eV (Figure 5b). The most intense PL band at 3.360 eV is the most common band observed in high-quality ZnO material [49–51]. It comes from the recombination of excitons bound to neutral donor impurities (D^0X), most probably related to diffusion of the Ga impurity from the GaAs core into the ZnO shell

during the ALD process in the investigated samples. The second band at 3.328 eV is also frequently observed in ZnO materials, and it was associated with excitonic recombination emission, which is, however, bound to structural defects, in contrast to higher energy PL bands associated either with excitons bound to shallow impurity centers, or to free excitons [49]. The third PL band at 3.310 eV was previously associated with donor-acceptor pairs (DAP) recombination [51,52]. The other lower energy PL bands are related to deeper, unidentified, point defects and complexes in the ZnO shell. One should note that the increase in the ZnO layer thickness with increasing the number of ALD cycles leads to the overall enhancement of the intensity of emission coming from ZnO as compared to that coming from the GaAs core, while it does not significantly influence on the ratios of PL bands intensity, when they are analyzed for the ZnO shell and the GaAs core separately, including those of polarized emission.

The measurements of the polarized luminescence revealed that the excitonic emission from the ZnO shell related to neutral donor bound excitons is polarized preponderantly in the radial direction of core–shell structure, while the emission associated with excitons bound to structural defects, as well as the other lower energy PL band, are polarized preponderantly along the nanowires (Figure 6b). Similarly, the high energy emission associated with shallow impurities in the GaAs core is polarized preponderantly in the radial direction of the core–shell structure, while the emission related to deeper recombination centers is polarized preponderantly along the nanowires (Figure 6a).

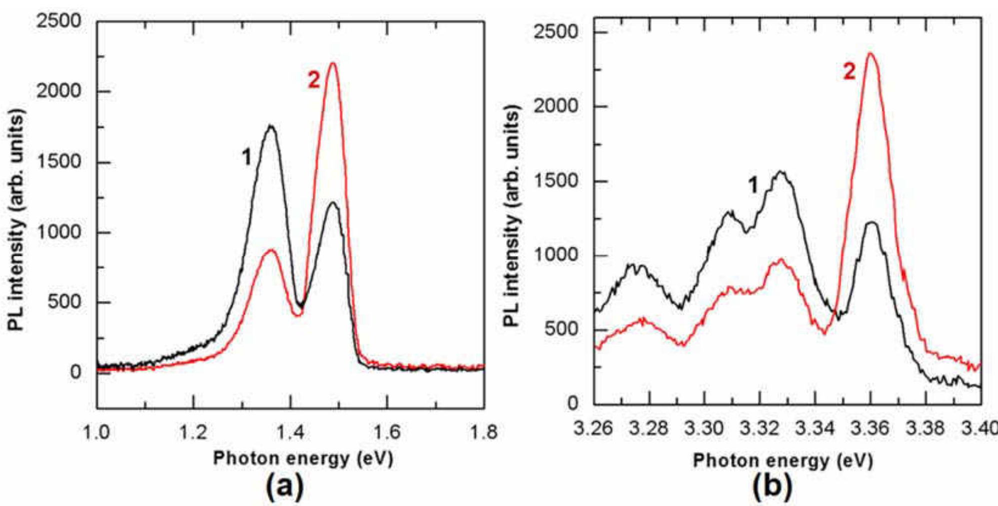

Figure 6. PL spectra of the GaAs core (**a**) and ZnO shell (**b**) measured at 10 K with the emission polarized along the nanowire axis (curve 1), and polarized in the radial direction (curve 2).

According to literature data, in most cases, the polarization anisotropy of the emission from semiconductor nanowires is related to their elongated geometry, and it is polarized along the axis direction [29,32]. According to the classical electromagnetic theory, this effect is considered to result from the large contrast in dielectric constants between the semiconductor nanowires and their surroundings.

However, the contribution from the symmetry of the crystal structure cannot be neglected since the polarized light emission is closely related to the symmetry of the wave functions. As a result, the polarizations of the excitonic emission from GaAs and InP nanowires with wurtzite (WZ) and zincblende (ZB) structures were found to be different. Although ZB nanowires exhibit strong polarization parallel to the nanowire axis, the WZ nanowires exhibit emission polarized perpendicular to the nanowire axis [30,31]. This behavior was interpreted in terms of the different selection rules for WZ and ZB crystal structures since they exhibit completely different symmetries. Similarly, the polarization of the near-band-edge photoluminescence in ZnO strain-free nanowires was found to be polarized predominantly perpendicular to the nanowire axis, and such a polarization

dependence was explained in terms of selection rules for excitonic transitions derived from the k·p theory for WZ ZnO [33].

In addition to the effects of contrast in dielectric constants and those of symmetry of the wave functions, strain also may have a significant effect on the emission polarization, especially on that related to defects or clusters. For instance, in contrast to the expected behavior of the near-band-edge emission polarization in ZB GaP, the luminescence related to the recombination of excitons bound at N-related clusters in coaxial GaNP nanowires with diameters ranging from 100 to 350 nm, as well as in core/shell GaP/GaNP structures was found to be strongly polarized in the direction perpendicular to the nanowire axis [34,35]. The effect was explained assuming that the N-related centers participating in emission experience tensile local strain. A similar effect was observed in coaxial GaAsN nanowires [36,37].

The effect of strain on the emission polarization was also demonstrated in GaN/AlGaN core/shell nanowires [38]. The emission of the uncoated strain-free GaN nanowires was found to be polarized perpendicular to the c-axis, as expected according to the crystal structure symmetry of the WZ GaN, while the GaN core compressively strained by the AlGaN shell exhibited a polarization parallel to the NW c-axis. This phenomenon was explained by the crossover of the valence sub-bands induced by strong strain, which resulted in the change of symmetry of the uppermost valence sub-band.

As concerns the emission polarization from the investigated coaxial GaAs/ZnO core/shell structures, the GaAs core is of ZB structure, according to data of Figure 2b, while the ZnO shell is of WZ structure, according to the position of the D^0X emission in Figure 5b. It is well documented that the PL spectrum of high-quality WZ ZnO crystals in the near-bandgap spectral range is always dominated by D^0X emission lines, each of them being attributed with a precision better than 1 meV to specific donor impurities to which excitons are bound (see for instance ref. [47]). These emission lines are fingerprints of the respective impurities. The I_8 line at 3.360 eV is related to the excitons bound to the Ga impurity [47]. The domination of the PL band at 3.360 eV in the shell grown by ALD is indicative of the WZ structure of ZnO. This band would not be observed in the PL spectrum of ZB ZnO. It is also known that the ZB phase of ZnO is much less stable at normal conditions than the WZ phase. On the other hand, the larger FWHM of the 3.360 eV band in the ZnO shell indicates that its quality is not as high as the quality of crystals produced by hydrothermal or vapor phase growth.

Therefore, the predominant polarization of the excitonic D^0X band in the WZ ZnO shell perpendicular to the nanowire axis suggests that the c-axis of the shell is oriented parallel with the nanowire axis, and the main effect in the polarization of this PL band comes from the ZnO WZ crystal structure symmetry, rather than from the contrast in dielectric constants. On the other hand, the predominant polarization of the lower energy PL bands, related to impurities or defects, along the nanowire axis may be governed by the contrast in dielectric constants.

Regarding the polarization of PL bands in the GaAs core, the polarization of the lower energy PL band at 1.360 eV along the nanowire axis may again be governed by the contrast in dielectric constants. The situation seems to be more complicated with the PL band at 1.486 eV. If an emission band associated with the recombination of excitons in the ZB GaAs would be observed in the spectrum, it would be polarized along the nanowire axis both from the point of view of excitonic emission selection rules and from the point on view of the contrast in dielectric constants. However, no excitonic emission was observed from the GaAs nanowire in the near-band-edge spectral region. On the other hand, the predominant polarization of the PL band at 1.486 eV perpendicularly to the nanowire axis may come from the specific microscopic structure of the defects involved in DA pair recombination or in the free-to-bound transitions, which may experience tensile local strain, similarly to the effects observed in coaxial GaNP and GaAsN nanowires, as well as in GaP/GaNP core/shell structures, as discussed above [34–37].

4. Conclusions

ZnO and TiO_2 coatings have been deposited by thermal atomic layer deposition on GaAs nanowires produced by anodization of (111)B GaAs substrates. The EDX analysis demonstrated the right proportions of the constituent elements in the composition of ZnO and TiO_2 coatings. The XRD analysis revealed the zinc–blende structure of the GaAs nanowires.

The PL emission from the GaAs core of coaxial core–shell structures was found to be dominated by a PL band related to carrier recombination via shallow donors and acceptors and a lower energy PL band associated with deeper recombination centers. The emission from the ZnO shell was dominated by a near band edge PL band coming from recombination of excitons bound to neutral donors D^0X and a lower energy band associated with recombination of excitons bound to structural defects. A series of lower energy PL band related to deeper recombination centers was also observed in the ZnO shell.

The analysis of polarized luminescence demonstrated that the D^0X emission from the ZnO shell is polarized predominantly perpendicular to the nanowire axis, while the lower energy PL band is polarized predominantly along the nanowire axis. The emission from the GaAs core associated with shallow impurities in the GaAs core was found to be polarized preponderantly in the radial direction of the core–shell structure, while the emission related to deeper recombination centers proved to be polarized preponderantly along the nanowires. The polarization of the observed PL bands was explained in terms of the contrast in dielectric constants, selection rules associated with crystal structure symmetry, and local strain related to specific microscopic structure of recombination centers involved in electronic transitions responsible for specific PL bands.

Author Contributions: Conceptualization, V.V.U., S.L. and E.V.M.; methodology, S.L., V.V.Z. and V.M.; validation, V.V.U. and K.N.; investigation, V.V.Z., V.M., S.L. and E.V.M.; writing—original draft preparation, V.V.U.; writing—review and editing, V.V.U., E.V.M. and I.M.T.; visualization, E.V.M. and V.M.; supervision, I.M.T. and K.N.; project administration, E.V.M. and I.M.T.; funding acquisition, I.M.T. All authors have read and agreed to the published version of the manuscript.

Funding: This research was funded by National Agency for Research and Development of Moldova under the Grants #21.00208.5007.15/PD "Micro- and nano-engineering of semiconductor compounds based on electrochemical technologies for electronic and photonic applications" and #22.80013.5007.4BL "Nano- and hetero-structures based on zinc oxide and A3B5 compounds for optoelectronics, photonics and biosensorics". The APC was funded by European Commission under the H2020 grant #810652 "NanoMedTwin".

Institutional Review Board Statement: Not applicable.

Informed Consent Statement: Not applicable.

Data Availability Statement: The data presented in this study are available on request from the corresponding authors.

Acknowledgments: E.V.M. acknowledges support from the Alexander von Humboldt Foundation (Bonn, Germany). V.M. acknowledges support from the German Academic Exchange Service for DAAD scholarship at IFW Dresden (Germany).

Conflicts of Interest: The authors declare no conflict of interest. The founding sponsors had no role in the design of the study; in the collection, analyses, or interpretation of data; in the writing of the manuscript, and in the decision to publish the results.

References

1. Wang, K. II-VI Core-Shell Nanowires: Synthesis, Characterizations and Photovoltaic Applications. PhD Thesis, University of New Orleans, New Orleans, LA, USA, 2012. Available online: https://scholarworks.uno.edu/td/1533 (accessed on 13 July 2022).
2. Ko, K.Y.; Kang, H.; Kim, J.; Lee, W.; Lee, H.S.; Im, S.; Kang, J.Y.; Myoung, J.-M.; Kim, H.-G.; Kim, S.-H.; et al. High Efficiency N-ZnO/p-Si Core–Shell Nanowire Photodiode Based on Well-Ordered Si Nanowire Array with Smooth Surface. *Mater. Sci. Semicond. Process.* **2014**, *27*, 297–302. [CrossRef]

3. Zhang, Y.; Wang, L.-W.; Mascarenhas, A. Quantum Coaxial Cables" for Solar Energy Harvesting. *Nano Lett.* **2007**, *7*, 1264–1269. [CrossRef] [PubMed]
4. Nduwimana, A.; Musin, R.N.; Smith, A.M.; Wang, X.-Q. Spatial Carrier Confinement in Core−Shell and Multishell Nanowire Heterostructures. *Nano Lett.* **2008**, *8*, 3341–3344. [CrossRef]
5. Pan, K.-Y.; Lin, Y.-H.; Lee, P.-S.; Wu, J.-M.; Shih, H.C. Synthesis of SnO_2-ZnO Core-Shell Nanowires and Their Optoelectronic Properties. *J. Nanomater.* **2012**, *2012*, 279245. [CrossRef]
6. Shao, D.; Sun, H.; Xin, G.; Lian, J.; Sawyer, S. High Quality ZnO–TiO_2 Core–Shell Nanowires for Efficient Ultraviolet Sensing. *Appl. Surf. Sci.* **2014**, *314*, 872–876. [CrossRef]
7. Hayden, O.; Greytak, A.B.; Bell, D.C. Core-Shell Nanowire Light-Emitting Diodes. *Adv. Mater.* **2005**, *17*, 701–704. [CrossRef]
8. Hiruma, K.; Yazawa, M.; Katsuyama, T.; Ogawa, K.; Haraguchi, K.; Koguchi, M.; Kakibayashi, H. Growth and Optical Properties of Nanometer-scale GaAs and InAs Whiskers. *J. Appl. Phys.* **1995**, *77*, 447–462. [CrossRef]
9. Gudiksen, M.S.; Lauhon, L.J.; Wang, J.; Smith, D.C.; Lieber, C.M. Growth of Nanowire Superlattice Structures for Nanoscale Photonics and Electronics. *Nature* **2002**, *415*, 617–620. [CrossRef] [PubMed]
10. Kim, H.-M.; Kang, T.W.; Chung, K.S. Nanoscale Ultraviolet-Light-Emitting Diodes Using Wide-Bandgap Gallium Nitride Nanorods. *Adv. Mater.* **2003**, *15*, 567–569. [CrossRef]
11. Grange, R. Nonlinear Optical Enhancement with Plasmonic Core-Shell Nanowires. In *Active Plasmonic Nanomaterials*; De Sio, L., Ed.; Pan Stanford Publishing Pte. Ltd: New York, NY, USA, 2015; Chapter 10; pp. 323–342.
12. Ramadurgam, S.; Lin, T.-G.; Yang, C. Tailoring Optical and Plasmon Resonances in Core-Shell and Core-Multishell Nanowires for Visible Range Negative Refraction and Plasmonic Light Harvesting: A Review. *J. Mater. Sci. Technol.* **2015**, *31*, 533–541. [CrossRef]
13. Mulla, R.; Dunnill, C.W. Core–Shell Nanostructures for Better Thermoelectrics. *Mater. Adv.* **2022**, *3*, 125–141. [CrossRef]
14. Musa, M.; Yasui, T.; Nagashima, K.; Horiuchi, M.; Zhu, Z.; Liu, Q.; Shimada, T.; Arima, A.; Yanagida, T.; Baba, Y. ZnO/SiO_2 Core/Shell Nanowires for Capturing CpG Rich Single-Stranded DNAs. *Anal. Methods* **2021**, *13*, 337–344. [CrossRef] [PubMed]
15. Liu, L.; Wang, H.; Wang, D.; Li, Y.; He, X.; Zhang, H.; Shen, J. ZnO@TiO_2 Core/Shell Nanowire Arrays with Different Thickness of TiO_2 Shell for Dye-Sensitized Solar Cells. *Crystals* **2020**, *10*, 325. [CrossRef]
16. Kim, H.W.; Yang, J.C.; Na, H.G.; Lee, C. Atomic Layer Deposition Coating of ZnO Shell for GaN–ZnO Core-Sheath Hetero-nanowires. *Appl. Surf. Sci.* **2011**, *257*, 9420–9424. [CrossRef]
17. Um, H.-D.; Moiz, S.A.; Park, K.-T.; Jung, J.-Y.; Jee, S.-W.; Ahn, C.H.; Kim, D.C.; Cho, H.K.; Kim, D.-W.; Lee, J.-H. Highly Selective Spectral Response with Enhanced Responsivity of N-ZnO/p-Si Radial Heterojunction Nanowire Photodiodes. *Appl. Phys. Lett.* **2011**, *98*, 033102. [CrossRef]
18. Kang, H.; Park, J.; Choi, T.; Jung, H.; Lee, K.H.; Im, S.; Kim, H. n-ZnO:N/p-Si Nanowire Photodiode Prepared by Atomic Layer Deposition. *Appl. Phys. Lett.* **2012**, *100*, 041117. [CrossRef]
19. Shen, X.; Yao, M.; Sun, K.; Zhao, T.; He, Y.; Chi, C.-Y.; Zhou, C.; Dapkus, P.D.; Lewis, N.S.; Hu, S. Defect-Tolerant TiO_2 -Coated and Discretized Photoanodes for >600 h of Stable Photoelectrochemical Water Oxidation. *ACS Energy Lett.* **2021**, *6*, 193–200. [CrossRef]
20. Royo, M.; De Luca, M.; Rurali, R.; Zardo, I. A Review on III–V Core–Multishell Nanowires: Growth, Properties, and Applications. *J. Phys. D Appl. Phys.* **2017**, *50*, 143001. [CrossRef]
21. Gao, X.; Fang, D.; Fang, X.; Tang, J.; Fang, F.; Li, J.; Chu, X.; Wang, X.; Wang, X.; Wei, Z. Surface Passivation of GaAs Using Atomic Layer Deposition Grown MgO. *Mater. Res. Express* **2015**, *2*, 095902. [CrossRef]
22. Czaban, J.A.; Thompson, D.A.; LaPierre, R.R. GaAs Core−Shell Nanowires for Photovoltaic Applications. *Nano Lett.* **2009**, *9*, 148–154. [CrossRef]
23. Monaico, E.V.; Morari, V.; Ursaki, V.V.; Nielsch, K.; Tiginyanu, I.M. Core–Shell GaAs-Fe Nanowire Arrays: Fabrication Using Electrochemical Etching and Deposition and Study of Their Magnetic Properties. *Nanomaterials* **2022**, *12*, 1506. [CrossRef] [PubMed]
24. Monaico, E.I.; Monaico, E.V.; Ursaki, V.V.; Honnali, S.; Postolache, V.; Leistner, K.; Nielsch, K.; Tiginyanu, I.M. Electrochemical Nanostructuring of (111) Oriented GaAs Crystals: From Porous Structures to Nanowires. *Beilstein J. Nanotechnol.* **2020**, *11*, 966–975. [CrossRef]
25. Monaico, E.; Tiginyanu, I.; Ursaki, V. Porous Semiconductor Compounds. *Semicond. Sci. Technol.* **2020**, *35*, 103001. [CrossRef]
26. Tiginyanu, I.; Monaico, E.I.; Monaico, E.V. Ordered Arrays of Metal Nanotubes in Semiconductor Envelope. *Electrochem. Commun.* **2008**, *10*, 731–734. [CrossRef]
27. Austin, A.J.; Echeverria, E.; Wagle, P.; Mainali, P.; Meyers, D.; Gupta, A.K.; Sachan, R.; Prassana, S.; McIlroy, D.N. High-Temperature Atomic Layer Deposition of GaN on 1D Nanostructures. *Nanomaterials* **2020**, *10*, 2434. [CrossRef] [PubMed]
28. Bachmann, J. *Atomic Layer Deposition in Energy Conversion Applications*; Bachmann, J., Ed.; Wiley-VCH Verlag GmbH & Co KGaA: Weinheim, Germany, 2017; p. 312.
29. Hoang, T.B.; Titova, L.V.; Jackson, H.E.; Smith, L.M.; Yarrison-Rice, J.M.; Kim, Y.; Joyce, H.J.; Jagadish, C. Imaging and Optical Properties of Single Core-Shell GaAs-AlGaAs Nanowires. In Proceedings of the 2006 Sixth IEEE Conference on Nanotechnology, Cincinati, OH, USA, 17–20 July 2006; Volume 1, pp. 116–118. [CrossRef]
30. Novikov, B.V.; Serov, S.Y.; Filosofov, N.G.; Shtrom, I.V.; Talalaev, V.G.; Vyvenko, O.F.; Ubyivovk, E.V.; Samsonenko, Y.B.; Bouravleuv, A.D.; Soshnikov, I.P.; et al. Photoluminescence Properties of GaAs Nanowire Ensembles with Zincblende and Wurtzite Crystal Structure. *Phys. Status Solidi RRL–Rapid Res. Lett.* **2010**, *4*, 175–177. [CrossRef]

31. Mishra, A.; Titova, L.V.; Hoang, T.B.; Jackson, H.E.; Smith, L.M.; Yarrison-Rice, J.M.; Kim, Y.; Joyce, H.J.; Gao, Q.; Tan, H.H.; et al. Polarization and Temperature Dependence of Photoluminescence from Zincblende and Wurtzite InP Nanowires. *Appl. Phys. Lett.* **2007**, *91*, 263104. [CrossRef]
32. Shan, C.X.; Liu, Z.; Hark, S.K. Photoluminescence Polarization in Individual CdSe Nanowires. *Phys. Rev. B* **2006**, *74*, 153402. [CrossRef]
33. Jacopin, G.; Rigutti, L.; Bugallo, A.D.L.; Julien, F.H.; Baratto, C.; Comini, E.; Ferroni, M.; Tchernycheva, M. High Degree of Polarization of the Near-Band-Edge Photoluminescence in ZnO Nanowires. *Nanoscale Res. Lett.* **2011**, *6*, 501. [CrossRef]
34. Buyanova, I.A.; Stehr, J.E.; Filippov, S.; Chen, W.M.; Tu, C.W. Novel GaP/GaNP Core/Shell Nanowires for Optoelectronics and Photonics. In Proceedings of the 2016 IEEE International Nanoelectronics Conference (INEC), Chengdu, China, 9–11 May 2016; p. 440. [CrossRef]
35. Filippov, S.; Sukrittanon, S.; Kuang, Y.; Tu, C.; Persson, P.O.Å.; Chen, W.M.; Buyanova, I.A. Origin of Strong Photoluminescence Polarization in GaNP Nanowires. *Nano Lett.* **2014**, *14*, 5264–5269. [CrossRef]
36. Buyanova, I.A.; Chen, W.M.; Ishikawa, F.; Tu, C.W. Novel GaNAs and GaNP-Based Nanowires—Promising Materials for Optoelectronics and Photonics. In Proceedings of the 2016 IEEE 16th International Conference on Nanotechnology (IEEE-NANO), Sendai, Japan, 22–25 August 2016; pp. 38–41. [CrossRef]
37. Buyanova, I.A.; Chen, W.M. Dilute Nitrides-Based Nanowires—a Promising Platform for Nanoscale Photonics and Energy Technology. *Nanotechnology* **2019**, *30*, 292002. [CrossRef] [PubMed]
38. Jacopin, G.; Rigutti, L.; Bellei, S.; Lavenus, P.; Julien, F.H.; Davydov, A.V.; Tsvetkov, D.; Bertness, K.A.; Sanford, N.A.; Schlager, J.B.; et al. Photoluminescence Polarization in Strained GaN/AlGaN Core/Shell Nanowires. *Nanotechnology* **2012**, *23*, 325701. [CrossRef] [PubMed]
39. Monaico, E.I.; Monaico, E.V.; Ursaki, V.V.; Tiginyanu, I.M. Evolution of Pore Growth in GaAs in Transitory Anodization Regime from One Applied Voltage to Another. *Surf. Engin. Appl. Electrochem.* **2021**, *57*, 165–172. [CrossRef]
40. Ku, C.-S.; Lee, H.-Y.; Huang, J.-M.; Lin, C.-M. Epitaxial growth of ZnO films at extremely low temperature by atomic layer deposition with interrupted flow. *Mater. Chem. Phys.* **2010**, *120*, 236–239. [CrossRef]
41. Yang, J.; Bahrami, A.; Ding, X.; Lehmann, S.; Kruse, N.; He, S.; Wang, B.; Hantusch, M.; Nielsch, K. Characteristics of ALD-ZnO Thin Film Transistor Using H_2O and H_2O_2 as Oxygen Sources. *Adv. Mater. Int.* **2022**, *9*, 2101953. [CrossRef]
42. He, S.; Bahrami, A.; Zhang, X.; Gonzalez Martinez, I.; Lehmann, S.; Nielsh, K. Effect of Powder ALD Interface Modification on the Thermoelectric Performance of Bismuth. *Adv. Mater. Technol.* **2022**, *7*, 2100953. [CrossRef]
43. Drygas, M.; Jelen, P.; Radecka, M.; Janik, J.F. Ammonolysis of polycrystalline and amorphized gallium arsenide GaAs to polytype-specific nanopowders of gallium nitride GaN. *RSC Adv.* **2016**, *6*, 41074. [CrossRef]
44. Kudo, K.; Makita, Y.; Takayasu, I.; Nomura, T.; Kobayashi, T.; Izumi, T.; Matsumori, T. Photoluminescence Spectra of Undoped GaAs Grown by Molecular-beam Epitaxy at Very High and Low Substrate Temperatures. *J. Appl. Phys.* **1986**, *59*, 888–891. [CrossRef]
45. Williams, E.W.; Barry Bebb, H. *Photoluminescence II: Gallium Arsenide*; Willardson, R.K., Beer, A.C., Eds.; Academic Press: Cambridge, MA, USA, 1972; Volume 8, Chapter 5; pp. 321–392.
46. Swaminathan, V.; Caruso, R.; Pearton, S.J. Photoluminescence from Annealed Semi-insulating GaAs Crystals: The 1.360 eV Band. *J. Appl. Phys.* **1988**, *63*, 2164–2167. [CrossRef]
47. Shin, K.C.; Kwark, M.H.; Choi, M.H.; Oh, M.H.; Tak, Y.B. Photoluminescence Investigation of the 1.356 eV Band and Stoichiometry in Undoped GaAs. *J. Appl. Phys.* **1989**, *65*, 736–741. [CrossRef]
48. Itoh, T.; Takeuchi, M. Arsenic Vacancy Formation in GaAs Annealed in Hydrogen Gas Flow. *Jpn. J. Appl. Phys.* **1977**, *16*, 227–232. [CrossRef]
49. Meyer, B.K.; Alves, H.; Hofmann, D.M.; Kriegseis, W.; Forster, D.; Bertram, F.; Christen, J.; Hoffmann, A.; Straßburg, M.; Dworzak, M.; et al. Bound Exciton and Donor–Acceptor Pair Recombinations in ZnO. *Phys. Stat. Sol. (B)* **2004**, *241*, 231–260. [CrossRef]
50. Ursaki, V.V.; Tiginyanu, I.M.; Zalamai, V.V.; Rusu, E.V.; Emelchenko, G.A.; Masalov, V.M.; Samarov, E.N. Multiphonon Resonant Raman Scattering in ZnO Crystals and Nanostructured Layers. *Phys. Rev. B* **2004**, *70*, 155204. [CrossRef]
51. Ursaki, V.V.; Tiginyanu, I.M.; Zalamai, V.V.; Masalov, V.M.; Samarov, E.N.; Emelchenko, G.A.; Briones, F. Photoluminescence and Resonant Raman Scattering from ZnO-Opal Structures. *J. Appl. Phys.* **2004**, *96*, 1001–1006. [CrossRef]
52. Ursaki, V.V.; Tiginyanu, I.M.; Zalamai, V.V.; Masalov, V.M.; Samarov, E.N.; Emelchenko, G.A.; Briones, F. Photoluminescence of ZnO Layers Grown on Opals by Chemical Deposition from Zinc Nitrate Solution. *Semicond. Sci. Technol.* **2004**, *19*, 851–854. [CrossRef]